

New Multi-Stage and Stochastic Mathematical Model for Maximizing RES Hosting Capacity— Part II: Numerical Results

Sérgio F. Santos, Desta Z. Fitiwi, *Student Member, IEEE*, Miadreza Shafie-khah, *Member, IEEE*, Abebe W. Bizuayehu, *Member, IEEE*, Carlos M. P. Cabrita, and João P. S. Catalão, *Senior Member, IEEE*

Abstract—A new multi-stage and stochastic mathematical model of an integrated distribution system planning problem is described in Part I. The efficiency and validity of this model are tested by carrying out a case study on a standard IEEE 41-bus radial distribution system. The numerical results show that the simultaneous integration of energy storage systems (ESSs) and reactive power sources largely enables a substantially increased penetration of variable generation (wind and solar) in the system, and consequently, reduces overall system costs and network losses. For the system, a combined wind and solar PV power of up to nearly three times the base-case peak load is installed over a three-year planning horizon. In addition, the proposed planning approach also considerably defers network expansion and/or reinforcement needs. Generally, it is clearly demonstrated in an innovative way that the joint planning of distributed generation, reactive power sources and ESSs, brings significant improvements to the system such as reduction of losses, electricity cost and emissions as a result of increased renewable energy sources (RESs) penetration. Besides, the proposed modeling framework considerably improves the voltage profile in the system, which is crucial for a normal operation of the system as a whole. Finally, the novel planning model proposed can be considered as a major leap forward towards developing controllable grids, which support large-scale integration of RESs.

Index Terms—Distributed generation, distribution network systems, energy storage systems, integrated planning, renewable energy sources, stochastic programming

I. NOMENCLATURE

A. Parameters

C_{ij}	Capital cost of line i - j (Euros)
V_{nom}	Nominal voltage (kV)
Z_{ij}	Impedance of line i - j (ohms)

B. Variables

V_i	Voltage at node i
-------	---------------------

This work was supported by FEDER funds through COMPETE and by Portuguese funds through FCT, under Projects FCOMP-01-0124-FEDER-020282 (Ref. PTDC/EEA-EEL/118519/2010) and UID/CEC/50021/2013. Also, the research leading to these results has received funding from the EU Seventh Framework Programme FP7/2007-2013 under grant agreement no. 309048. S.F. Santos gratefully acknowledges the UBI / Santander Totta doctoral incentive grant in the Engineering Faculty.

S.F. Santos, D.Z. Fitiwi, M. Shafie-khah, A.W. Bizuayehu and J.P.S. Catalão are with INESC TEC and the Faculty of Engineering of the University of Porto, Porto 4200-465, Portugal, also with C-MAST, University of Beira Interior, Covilhã 6201-001, Portugal, and also with INESC-ID, Instituto Superior Técnico, University of Lisbon, Lisbon 1049-001, Portugal (e-mails: sdfsantos@gmail.com, dzf@ubi.pt, miadreza@gmail.com, buzeabebe@gmail.com, catalao@ubi.pt).

C.M.P. Cabrita is with CISE - Electromechatronics Systems Research Centre, University of Beira Interior, Covilha, Portugal (cabrita@ubi.pt).

$x_{g,i,t}, x_{es,i,t}, x_{c,i,t}, x_{k,t}$ Investment variables for DG, energy storage system, capacitor banks and distribution lines

II. INTRODUCTION

ELECTRICAL distribution systems are expected to accommodate large-scale DGs in the coming years because it is now widely accepted that DGs bring wide-range benefits to the system. In the companion paper, the main drivers, the challenges and the limitations of integrating large-scale DGs in distribution systems as well as the technical solutions ahead for alleviating the side-effects of such integration are presented. Distribution network systems (DNSs) are especially expected to be equipped with smart-grid enabling technologies that significantly enhance the scale of DGs integrated into the system (renewables, in particular) by substantially reducing their negative impacts so that the system integrity, stability and power quality are maintained at standard levels. To this end, it is highly required to coordinate DG integration planning with the deployment of different smart-grid enabling technologies such as reactive power sources, advanced switching and storage devices.

A description of a multi-stage and stochastic mathematical model is presented in Part I of this paper. The developed model simultaneously determines the optimal sizing, timing and placement of ESSs and reactive power sources as well as that of RESs in distribution networks. The ultimate goal of this optimization work is to maximize the RES power absorbed by the system at a minimum cost while maintaining the power quality and stability at the required/standard levels.

In addition to the three novel contributions presented in the companion paper (Part I), this part includes two additional novel contributions:

- A comprehensive analysis considering RES-based DGs with and without reactive power support capabilities. The optimal power factor settings are estimated for both cases.
- A heuristic strategy for reducing the combinatorial solution search space in relation to the optimal placement of DGs, ESSs and reactive power sources.

The remainder of this paper is organized as follows. Simulation results are presented and discussed in III. The final section presents some conclusions and implications drawn from the simulation results.

III. CASE STUDY, RESULTS AND DISCUSSION

A. System Data and Assumptions

The radial DNS, shown in Fig. 1, is used to test the proposed planning model. The total active and reactive loads of the system are 4.635 MW and 3.25 MVar, respectively. The nominal voltage of the system is 12.66 kV. Information regarding network and demand data is provided in [1]. This system is selected for our case study because it is highly lossy and not properly compensated. The voltage profile in the base case, obtained from power flow analysis, can be found in [2]. For the sake of clarity, these nodal voltages are also reproduced in Fig. 2 in the form of cumulative distribution function. Note that these results correspond to a substation power factor of 0.894 and with no lower voltage limit restrictions imposed on the system. As it can be observed in Fig. 2, more than 70% of the nodal voltages are below 0.95 per unit. However, this contradicts with the minimum voltage set in distribution systems (often above this limit) for stability reasons. Running power flows by imposing the minimum voltage limits while keeping the substation power factor at 0.894 leads to infeasibility. This may be because of the high reactive power requirement in the system, which has to be provided by the substation given the fact that there the system is not well-compensated. Reducing the power factor of the substation to 0.706 results in a feasible solution but around 40% of the voltages are yet very close to the minimum value.

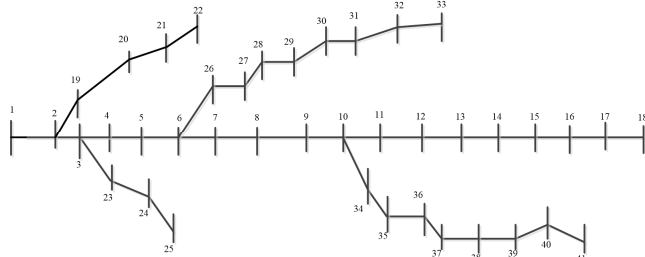


Fig. 1. Single-line diagram of the IEEE 41-bus distribution network system.

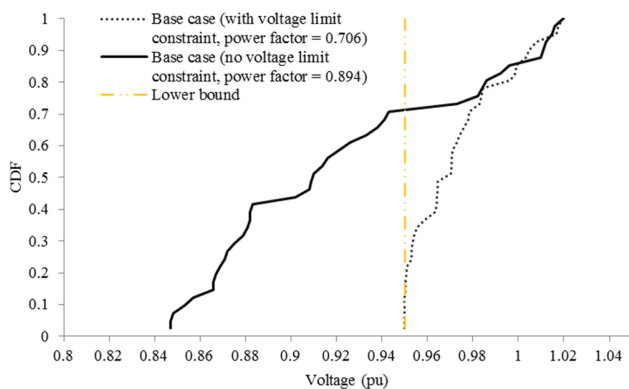


Fig. 2. Cumulative distribution function (CDF) of voltages in the base case.

The following assumptions are made when carrying out the simulations:

- A 3-year planning horizon is considered, which is divided into yearly decision stages.
- The interest rate is set to 7%.
- Electricity price at the substation follows the same trend as the demand i.e. electricity price and demand profile are 100% correlated.

- For the sake of simplicity, maintenance costs are taken to be 2% of the corresponding investment costs.
- The expected lifetime of capacitor banks and energy storage systems is assumed to be 15 years [3], [4], while that of DGs and feeders is 25 years [5].
- A 5% voltage deviation is considered to be the maximum allowable deviation from the nominal value that one can have in the system nodes i.e. $-0.95V_{nom} \leq V_i \leq 1.05V_{nom}$.
- The power transfer capacity of all feeders is assumed to be 6.986 MVA.
- All big-M parameters in the model formulation are set to 10, which is sufficiently higher than the power transfer capacity of all feeders.
- When linearizing quadratic terms in the developed planning model, the number of partitions is set equal to 5. This balances well accuracy with computation burden, as concluded in [6].
- The efficiency of the bulk ES is assumed to be 90%.
- The unit cost of capacitor banks is assumed to be €25/kVAr.
- The size of the minimum deployable capacitor bank is considered to be 0.1 MVar.
- The investment cost of a 1.0 MW bulk ES, whose energy reservoir is 5 MWh, is considered to be 1.0 M€.
- The emission rate of power purchased is arbitrarily set equal to 0.4 tCO₂e/MWh.
- The investment cost of a given feeder is assumed to be directly proportional to its impedance i.e. $C_{ij} = \alpha * Z_{ij}$ where the proportionality constant α is 10,000 €/Ω.
- Wind and solar type DGs, each with a 1 MW installed capacity, are considered as potential candidates to be deployed in the system. The investment costs of these generators are assumed to be 2.64 M€ and 3.00 M€, respectively.
- Electricity demand in the first, the second and the third planning stages is assumed to be 5%, 10% and 15% higher than the demand in the base-case, respectively.
- The emission prices in the first, second and third stages are set to 25, 45 and 60 €/tCO₂e, respectively.
- Variable power generation sources (wind and solar, in particular) are assumed to be available in every node. This assumption emanates from the fact that distribution networks span over a small geographical area. Hence, the distribution of resources in this area can be considered to be the same.
- The substation node (node 1) is considered as a reference; hence, its voltage magnitude and angle are set to $1.02 * V_{nom}$ and 0, respectively.
- The cost of unserved energy is set to 3000 €/MWh.

B. A Strategy for Reducing Combinatorial Solution Search Space

In the case study presented above, all nodes in the system are assumed to be candidates for the placement of DGs, ESS and capacitor banks. However, this is not possible when the planning work is carried out on large-scale DNSs because the size of the problem becomes huge as a result of combinatorial explosion, rendering difficulty in solving the problem. Owing to this fact, the potential candidate nodes are often

predetermined either arbitrarily or using some criteria for the selection such as the level of load, availability of resources, etc. For example, the possible connection points of RES-based DGs are often known a priori based on the availability of primary energy sources (such as wind speed and solar radiation). However, the variation in the availability of wind speed and solar radiation among the connection points in the DNS is not expected to be significant because it normally spans over a geographically small area, where the weather situation is more or less the same.

Here, we show how the combinatorial solution search space can be substantially reduced using a simple heuristic method. The method is based on solving a relaxed version of the original problem. This is done by treating all (normally integer) investment variables as continuous ones, with the exception of the line reinforcement variables. This effectively means fractional investment decisions are allowed. The method here works by first establishing a threshold for each fractional investment solution (i.e., corresponding to DGs, ESS and capacitor banks).

Then, those nodes whose corresponding values of investment solutions are lower than the preset thresholds are neglected. For instance, consider the investment solution of the relaxed problem corresponding to ESS at each node, as shown in Fig. 3. In this case, the threshold is arbitrarily set to 0.15. As we can see, for most of the nodes, the investment values corresponding to ESS fall below this threshold. Only those values at the following nodes are significant: {14, 18, 29, 30, 31, 32, 37, 38, 39, 40}. This set of nodes is hence considered as the most likely locations in the system for ESS placements in the full stochastic mixed integer linear programming (S-MILP) model. It should be noted that such a reduction in possible connection points (from 41 to 10) substantially speeds up the solution process as a result of the combinatorial solution search space. Similarly, the reduced set of nodes for possible capacitor and DG connections are obtained by arbitrarily considering 1.0 and 0.2 as the respective thresholds, as illustrated in Figs. 4 and 5. In this case, {7, 8, 14, 24, 25, 29, 30, 31, 32, 37, 38, 39, 40} is the reduced set of nodes for capacitor bank connections, while that of DGs is {7, 8, 14, 18, 25, 29, 30, 31, 32, 37, 38, 39, 40}. Note that the procedure/criterion for setting the threshold in each case is an open question. It may also depend on the nature and the size of the system under consideration. In general, each threshold should be carefully set to a sufficiently low value so that relevant information is not lost (i.e. potential candidate nodes are not excluded). The thresholds in this work are set based on the intuition that those nodes, whose investment values are zero or close to zero, are less likely to appear in the final set of solutions.

A deterministic planning model (i.e. considering a single scenario corresponding to the average demand, wind and solar PV power output profiles) is used to evaluate the performance of the heuristic approach proposed here. The results of the deterministic model obtained by applying the heuristic method are compared with that of the “brute force” model i.e. without reducing the set of candidate nodes for DG, ESS and capacitor placements. The investment decisions obtained are the same in both cases but the computational requirements substantially differ from one another. The proposed method helps to

significantly reduce the combinatorial solution search space, and thus the computational effort by more than sevenfold. In general, for distribution networks of this size, the proposed heuristic approach may not be needed or a short-list of candidate nodes for DG, ESS and capacitor placement may be made available based on expert knowledge. The problem is tractable without the need of reducing the solution search space as shown in Table I. However, one cannot rely on expert knowledge when the planning involves large-scale distribution network systems. In such problems, and when there is a lack of adequate computing machine, it is critical to employ mechanisms that reduce the combinatorial solution search space. In our case, this relates to reducing the number of candidate nodes for allocating DGs, ESSs and capacitor banks.

For the case study considered in this paper, the results obtained by applying the heuristic approach are the same as those obtained with the “brute-force” model which treats every node as a candidate for placement of DGs, ESSs and capacitor banks. However, it should be noted that since the proposed method is heuristic, its performance can be different for different systems. The approach contributes a lot to the solution process; yet, the conclusions drawn from the test results in this work cannot be generalized. The authors acknowledge that vital information could be excluded when setting the threshold to reduce the number of candidate nodes. For instance, even if the investment solution at a certain node in the relaxed problem is close to zero, the node could still be feasible for DG, ESS and/or capacitor placement in the full-scale stochastic model. As a final remark, careful analysis of the system under consideration is required when applying the reduction method proposed in this paper.

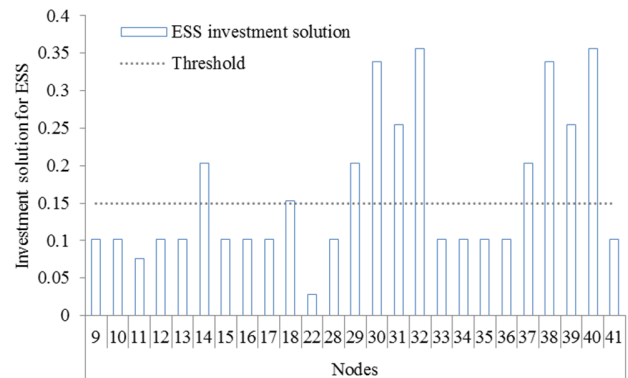


Fig. 3. Decision variable for ESS at each node (last stage).

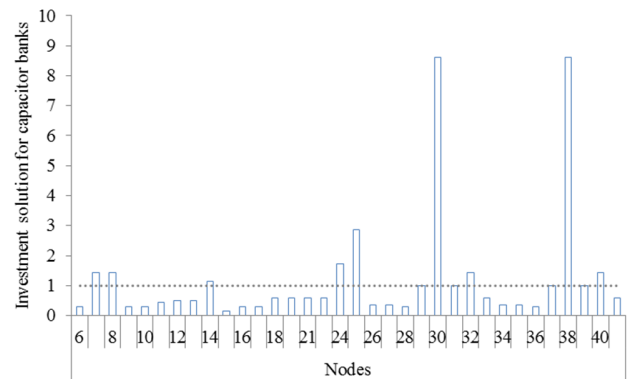


Fig. 4. Investment solution for capacitor banks at each node (last stage).

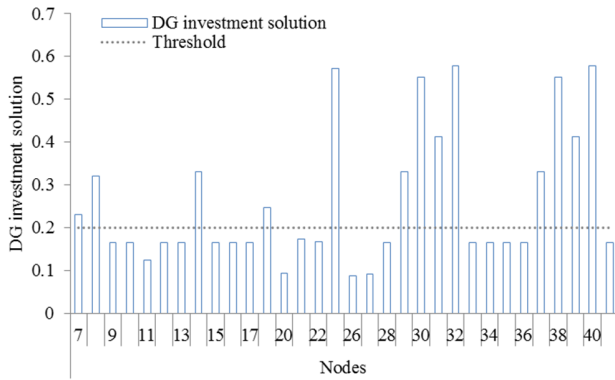


Fig. 5. Investment solution for DGs at each node (last stage).

Table I compares the size of the problem before and after applying the heuristic combinatorial solution search space reduction method. We can see that the combinatorial solution search space is reduced from 2^{720} to 2^{387} , and this also helps to reduce the number of equations and continuous variables by more than 18% and 13%, respectively.

TABLE I
COMPUTATIONAL SIZE OF THE OPTIMIZATION PROBLEM

	Brute-force	Reduced
Number of equations	11,032,828	9,039,895
Number of variables	9,315,028	8,100,028
Discrete variables	720	387
Simulation time (hours)	26.2	3.7

C. Results and Discussion

Intermittent power generation sources such as wind and solar PV type DGs normally operate with a fixed lagging power factor [7]. In other words, such generators “consume” reactive power, instead of “producing” and contributing to the voltage regulation in the system (also known as reactive power support). For instance, wind turbines installed in power systems throughout the world are predominantly based on asynchronous generators (also known as induction generators). As mentioned above, one of the typical characteristics of such machines is that they always “consume” reactive power. Because of this, such wind turbines are often operated at a constant power factor. It is well-known that, in power systems, voltage regulation has been traditionally supported by conventional (synchronous) generators.

However, this is likely to change in the near future given the upward trend of integrating such resources in power systems. Variable power generators, equipped with reactive power support devices predominantly based on power electronics, are expected to be deployed to enhance their capability to provide reactive power when it is needed in the system. We have carried out the system expansion for two cases: DGs without and with reactive power support capabilities.

The first case assumes that all wind and solar PV generators always “consume” reactive power, and they are operated at a fixed lagging power factor pf_g . The reactive power Q_g , in this case, is given by the product of the actual production of the DG and the tangent of the phase angle

between voltage and current i.e. $Q_g = P_g * \tan(\cos^{-1}(pf_g))$. In other words, the ratio between active and apparent power is kept constant. For instance, asynchronous (induction) generators used in conventional wind turbines have such characteristics. Most solar PVs also “consume” reactive power because of the power electronics involved. The second case assumes that all wind and solar PV generators have the capability to “produce” or “consume” reactive power depending on the operational situations, in a “similar” way as conventional power generators. For instance, a variable generation source g in this category is capable of operating between pf_g lagging power factor (reactive) to pf_g leading power factor (capacitive) depending on system requirements i.e. $-P_g * \tan(\cos^{-1}(pf_g)) \leq Q_g \leq P_g * \tan(\cos^{-1}(pf_g))$ where P_g is the actual power output of the generator at a particular time and Q_g is the reactive power “produced” or “consumed”. The simulation results corresponding for each case are discussed as follows.

1) Considering DGs Without Reactive Power Support

The power factor of wind and solar PV type DGs is varied from 0.8 lagging power factor (reactive) to unity power factor [7]. This means such DGs consume reactive power all the time. The system is expanded considering this case, and the expansion results are discussed below.

The optimal solution for capacitor banks, DGs and bulk ES in the system are shown in Tables II through IV, respectively. In general, majority of the investments are made in the first stage. This is because the NPV of operation and emission costs are higher in the first stage than those in any of the subsequent stages. This makes it attractive to invest more in renewables in the first stage than in the other stages so that these costs are drastically reduced.

As we can see in Table II, the optimal location of capacitor banks mostly coincides with high load connection points (nodes) as well as with those closer to the end nodes. This is expected from the system operation point of view because capacitor banks are required at such nodes to meet the reactive power requirements and thus keep the corresponding voltages within allowable operational limits. Otherwise, the voltages are expected to drop at these nodes without a reactive power compensation mechanism put in place. As shown in Table II, the total size of investment in capacitor banks required throughout the planning horizon varies from 3.7 MVAR at unity power factor to 12.5 MVAR at 0.8 lagging power factor, most of which are installed in the first stage of the planning horizon.

As shown in Table IV, more investments are made in wind than in solar PV type DGs. This is because of the higher capacity factor of potential wind power generators compared to solar PV ones. In general, the total MW of DG power installed at each node throughout the planning horizon is shown in Table IV.

Here, it can be observed that the overall optimal size of DGs integrated into the system remains more or less the same regardless of the power factor setting. However, the optimal placements of the installed DGs are in some cases different for different power factor settings. It is worth mentioning here that majority of these investments are made in the first stage of the planning horizon. This may be due to the absence of

investment constraints or because the NPV cost of operation and emissions is higher in the foremost stages than in the following ones.

TABLE II
OPTIMAL INVESTMENT SOLUTION OF CAPACITOR BANKS AT THE END OF THE PLANNING HORIZON

Location	Power factor				
	1.0	0.95	0.9	0.85	0.8
7	6	9	13	3	7
8	1	0	0	5	11
14	3	13	16	20	20
24	0	1	2	2	10
25	3	3	3	9	10
29	0	3	1	12	20
30	8	10	13	9	10
31	1	2	1	7	1
32	2	5	7	2	2
37	1	1	1	8	4
38	9	20	13	8	20
39	1	1	10	7	8
40	2	6	2	2	2
Total MVar	3.7	7.4	8.2	9.4	12.5

TABLE III
OPTIMAL INVESTMENT SOLUTION OF DGs AT THE END OF THE PLANNING HORIZON

DG type	Location	Power factor				
		1.0	0.95	0.9	0.85	0.8
PV	29	0	0	0	1	0
PV	32	0	1	0	0	0
PV	38	1	1	0	0	1
PV	39	0	0	1	0	0
Wind	7	0	1	1	0	1
Wind	14	3	3	3	3	3
Wind	25	0	0	0	1	1
Wind	29	0	1	0	1	3
Wind	30	2	0	1	0	0
Wind	31	0	0	0	1	0
Wind	32	1	1	1	0	0
Wind	37	0	0	0	1	0
Wind	38	2	1	1	0	1
Wind	39	0	1	1	1	1
Total (MW)		9	10	9	9	11

TABLE IV
OPTIMAL INVESTMENT SOLUTION OF ESS AT THE END OF THE PLANNING HORIZON

Location	Power factor				
	1.00	0.95	0.90	0.85	0.80
14	2	2	2	2	2
30	0	1	2	0	0
31	0	0	0	1	0
32	2	1	1	0	2
38	2	0	0	2	0
40	0	1	1	1	1
Total (MW)	6	5	6	6	5

The results in Tables II through IV show the strong relationships among the optimal investment solutions. For instance, Table II indicates that the lower the power factor is, the higher the investment requirement in capacitor banks is. This is due to the increasing reactive power consumption by the DGs. Unlike in capacitor banks, the total amount of DGs and ESSs installed in the system (see Tables III and IV) do not show significant variations with the reactive power settings. This is an indication that capacitor banks play a vital role in

maintaining system integrity and stability as well as ensuring essentially the same level of DG integration regardless of the power factor setting. The results in Tables III and IV also reveal that, the bulk ESSs and DGs in particular are optimally located close to one another. This is mainly because placing the ESSs close to the RES-based DG connection points ensures optimal utilization and integration of such DGs in the system.

It is well known that bulk ESS can bring significant benefits such as load following, power stability improvements, and enhancing the dispatchability of RESs from the system operator’s point of view according to their operation modes. Likewise, the optimal deployment of capacitor banks also brings substantial benefits to the system. The combination of all these entirely helps one to dramatically increase the size of RES-based DGs (up to 11 MW) that can be integrated into the system without violating system constraints. The optimal size of DGs would, otherwise, be limited to less than 3 MW [8]. It is interesting to see here that the integration of ESSs and capacitor banks has such a dramatic impact on the level of DG integration. This is due to the fact that ESSs and capacitor banks bring about significant flexibility and control mechanism to the system. Substantial improvements in voltage controllability are also clearly visible in Figs. 6 and 7 corresponding to a power factor setting of 0.95. These figures show the voltage deviation profiles at each node with the selected operational situations (which can alternatively be understood as “long hours”) without and with system expansion, respectively. In the base case (shown in Fig. 6), one can see that some of the node voltage deviations (especially those at the extreme nodes) tend to be very close to the minimum allowable limit. On the contrary, all node voltages largely stay very close to the nominal one (with an average deviation of approximately 1.5 %), leaving significant margins to the operational limits. Alternatively, Fig. 8 conveniently shows the variance of the voltage deviations at each node. It is also evident to see here that the variance of most of the deviations is very low. The highest variances at nodes 20 to 22 are due to high impedance of the feeder connected between nodes 19 and 20. The same reasoning explains the relatively high variances in the voltage deviations between nodes 13 and 18. However, these variances are negligible when put in perspective with the square of maximum deviation, i.e. $(2 * \Delta V^{max} / V_{nom})^2$, which in this case is approximately $(2 * 0.05)^2 \approx 1.0\%$. In general, such a substantial improvement in voltage controllability has come from the combined effect of expansion decisions in DGs, ESSs and capacitor banks.

Other important aspects in this expansion analysis are related to the impact of system expansion on the network losses and investments. Fig. 9 shows a comparison of the network losses in the base case and with expansion for every operational state. We can see a significant reduction in network losses in the system (by nearly 50% on average) after the expansion planning is carried out. This is one of the major benefits of integrating DGs in the system. Concerning investments in lines, in this particular case study, not a single feeder is selected for reinforcements. This clearly indicates that a properly designed integration of DGs leads to substantial network reinforcement/investment deferrals.

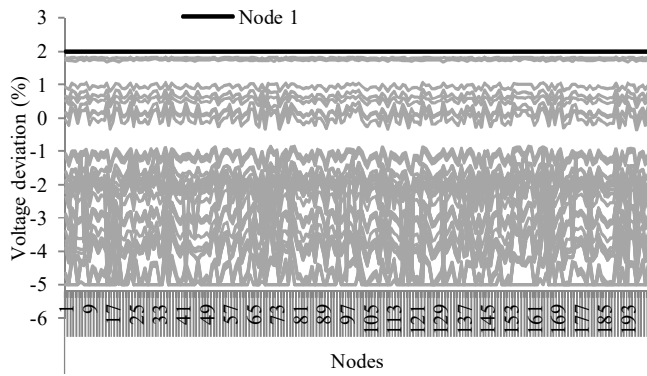


Fig. 6. Profiles of voltage deviations without system expansion in the first stage.

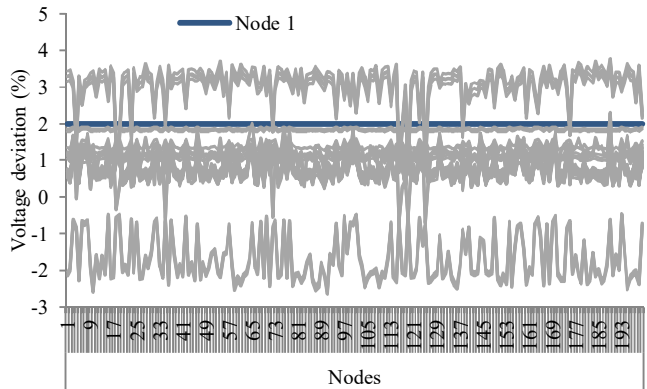


Fig. 7. Profiles of voltage deviations at each node after expansion in the first stage.

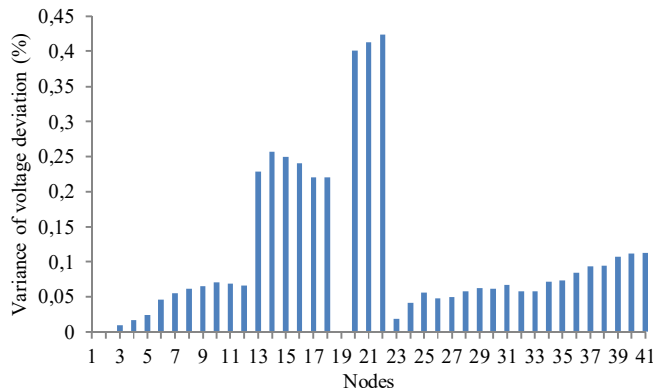


Fig. 8. Variance of voltage deviations at each node as a result of variations in system operational states.

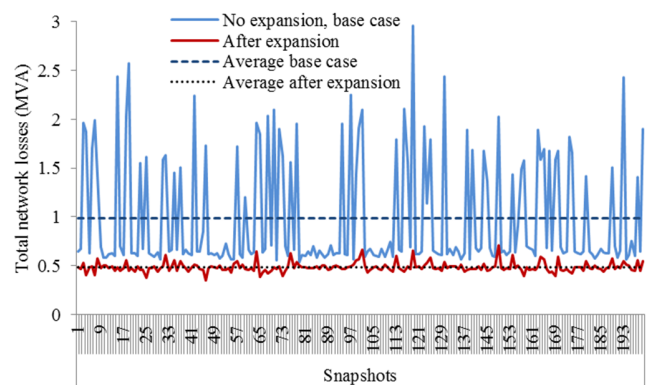


Fig. 9. Network losses with and without system expansion (first stage).

TABLE V
VALUES OF SYSTEM VARIABLES WITH VARYING POWER FACTOR OF RES-BASED DGs

	Power factor	1.0	0.95	0.9	0.85	0.8	
Total energy production (MWh)		179329	175545	176024	178848	172037	
RES energy production share (%)	Wind	44.00	45.08	45.23	46.31	46.90	
	PV	0.71	2.02	4.31	2.39	1.96	
	Wind+PV	44.71	47.10	49.54	48.69	48.86	
Cost terms (M€)	Investment cost	33.94	35.88	34.35	35.69	38.91	
	Maintenance Cost	9.47	9.47	9.53	9.43	10.10	
	Emission Cost	9.44	8.10	8.08	8.12	6.76	
	Energy Cost	29.31	27.10	27.65	27.20	25.22	
Total cost (M€)		82.16	80.55	79.61	80.44	80.99	
Investment decisions	Storage (MW)	6	5	6	6	5	
	Capacitor (MVar)	3.7	7.4	8.2	9.4	12.5	
	DG (MW)	9	10	9	9	11	
	Line reinforcements		1	3	1	1	2
Average active power losses in stage 1 (MW)		0.448	0.440	0.430	0.441	0.448	
Average reactive power losses in stage 1 (MVar)		0.339	0.745	0.983	1.098	1.602	

Table VI summarizes the analysis results, showing the variations of different system variables for different values of power factors. Fig. 10 also conveniently plots the trend of wind as well as combined solar and wind energy production shares for different power factor values. The results in this figure show that the wind energy production share increases when the power factor is further reduced. This may be because of the inherent characteristics of wind power production. In most cases, the availability and strength of wind speed is higher during low demand consumption hours (during night and early morning hours for instance) and lower during peak hours. This is directly related to the power production. During valley hours, the wind turbines act as reactive power sinks.

In relation to this, it can generally be observed that the lower the power factor is, the higher the reactive power consumed by the wind turbines. This may improve system efficiency and pave the way to higher wind power production. Hence, this may justify their increasing share of power production with decreasing power factor.

Contrary to the case with wind type DGs, the peak power production of solar PV based DGs occur around the peak hours of consumption. This means that, unlike the wind type DGs, their contribution to the system as reactive power sinks during valley hours is limited. Hence, as can be seen in Fig. 11, the optimal power factor setting for such DGs seems to be 0.9. In general, this also seems to be the optimal power factor setting for the system because this results in the highest share of combined wind and solar PV energy production (see Fig. 10). Besides, as can be seen in Table V, the lowest overall cost (79.61 M€) as well as the lowest active power losses (0.430 MW) are achieved when the power factor is set to 0.9.

As shown in Table V, the amount of installed reactive power sources (capacitor banks, in this case) as well as the reactive power losses in the system increase with decreasing power factor. This is expected because the lower the power factor is, the higher the reactive power requirement of the DGs is. Transporting the reactive power generated by such reactive power sources increases reactive power losses in the system.

The impact of varying power factor on the voltage profile in the system is also investigated. Figs. 12 and 13 illustrate the changes in the voltage profiles as a result of changing the

power factor during peak and valley hours, respectively. In both cases, there are no significantly visible variations in voltage profiles regardless of the power factor settings, except for some nodes as in Fig. 13. The average voltage deviations at each node for different power factor settings are also shown in Fig. 14.

In general, based on the results in Figs. 13 and 14, there is no clear indication to say that one power factor setting is better than the other; it can be observed that what is deemed good for one node may be “bad” for another one. However, it is worth mentioning here that the voltage profiles are significantly improved as a result of simultaneously integrating DG, ESS and capacitor banks. The voltage deviations for those nodes, where DGs and capacitor banks are connected to, seem to be higher in absolute terms; yet, they remain within the permissible range.

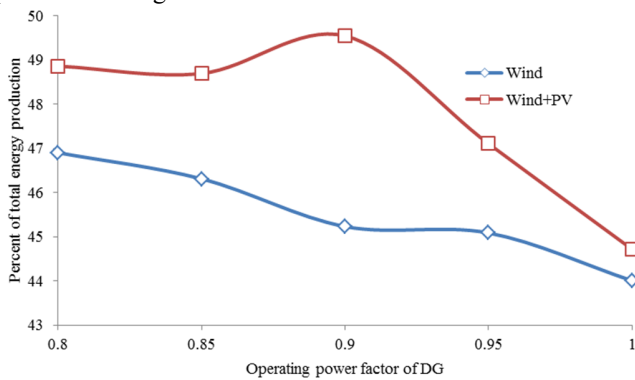


Fig. 10. Evolution of solar and wind energy production share with varying power factor.

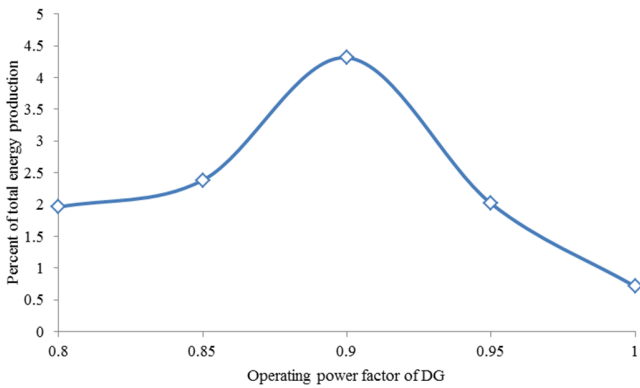


Fig. 11. Evolution of solar PV energy production share with varying power factor.

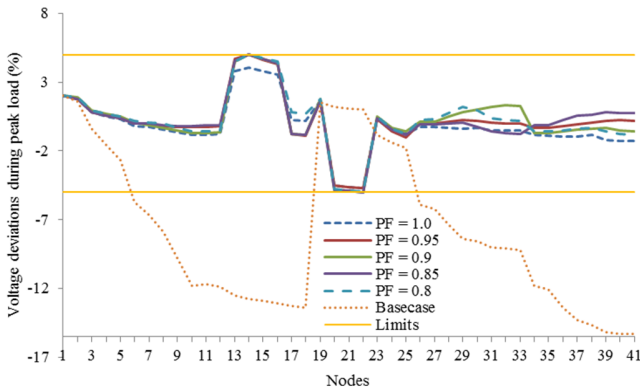


Fig. 12. Voltage deviation at each node during peak demand hour for different power factor values.

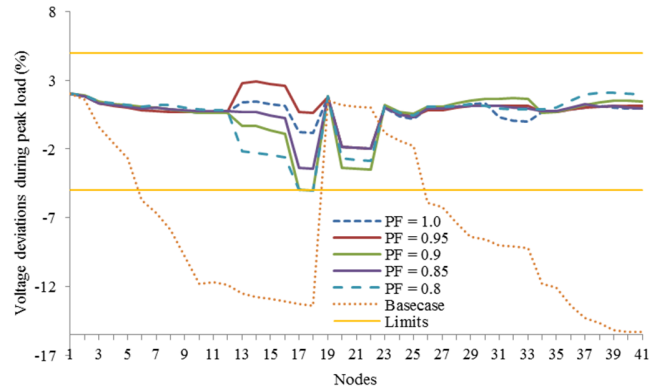


Fig. 13. Voltage deviation at each node during valley hour for different power factor values.

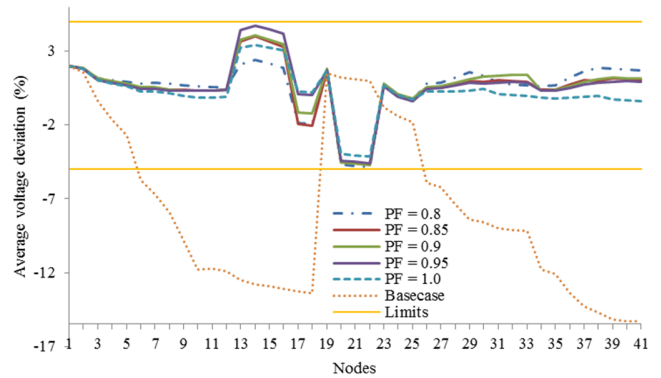


Fig. 14. Average voltage deviations at each node for different power factor values.

2) Considering DGs With Reactive Power Support

Nowadays, RES-based DGs (wind and solar types) are required to adhere to certain grid codes such as reactive power support, voltage ride through, etc. to alleviate the negative impacts of integrating such DGs in the system.

Examples in this case are doubly fed induction generator (DFIG) based wind turbines and voltage-source inverter (VSI) based PV generators. In some systems, the grid codes are already being enforced, and consequently wind/solar PV farms are required to operate from 0.95 lagging to 0.95 leading power factor [9].

For the analysis in this section, wind and solar PV type DGs with reactive power support capability are considered in the simulations. The power factor is varied to investigate its effects on selected system variables, and the results are summarized in Table VI. The results here show that the optimal power factor setting for the wind type DGs seems to be 0.95 because this leads to the highest wind energy production level (47.13%) compared to any other setting. This is also clearly shown in Fig. 15. The combined share of wind and solar PV energy production also peaks when the power factor is set to 0.95, as depicted in Fig. 15. From Table VI and Fig. 16, one can see that the overall cost (which is the sum of investment, maintenance, emission and energy costs) is the lowest at the same power factor (79.40 M€). The lowest active power losses seem to however occur at a power factor of 0.9.

The profiles of average voltage deviations at each node corresponding to different power factor settings are shown in Fig. 17. Fig. 18 also depicts the voltage deviations at each node corresponding to the valley hour of electricity

consumption. One can see that there are no significant differences in these profiles, except for nodes where the distributed energy resources (DG, ESS and reactive sources) are connected to. The voltage variations at these nodes with the changes in power factor settings can be explained by the fact that the amount of each distributed energy resource installed at these nodes is different for different power factor values (see Table VI).

TABLE VI
VALUES OF SYSTEM VARIABLES WITH VARYING POWER FACTOR OF RES-BASED DGs

	Power factor	1.00	0.95	0.9	0.85	0.80
Total energy (MWh)		179329	179329	179851	175527	176027
RES energy production share (%)	Wind	44.00	47.13	42.90	42.76	41.41
	PV	0.71	0.00	1.91	1.91	3.40
Cost terms (M€)	Investment cost	33.94	33.18	33.09	31.68	32.56
	Maintenance Cost	9.47	9.98	8.92	9.00	8.48
	Emission Cost	9.44	8.07	9.38	9.44	9.40
	Energy Cost	29.31	28.17	29.04	29.49	28.76
Total cost (M€)		82.16	79.4	80.43	79.61	79.2
Investment decisions	Storage (MW)	6	8	5	6	4
	Capacitor (MVar)	3.7	3.4	3.3	7.9	5
	RES (MW)	9	8	9	8	9
	Line reinforcements	1	1	8	0	7
Average active power losses in stage I (MW)		0.448	0.437	0.425	0.427	0.448
Average reactive power losses in stage I (MVar)		0.339	0.629	0.797	0.904	1.06

Comparing the results in Tables V and VI, one can observe that the consideration of reactive power support capability in the planning process results in a slight reduction in the objective function value (overall cost) and about 5% increase in the wind energy production share. In addition, as illustrated in Tables V and VI, when DGs with reactive power support capability are considered, losses in the system are lower than when DGs without such capability are instead installed.

3) Impact of Wind Turbine and Solar PV Size Selections on the Results

To carry out this analysis, the wind and solar PV DGs are assumed to operate from 0.95 lagging to 0.95 leading. Two wind turbine sizes, with 1.0 MW and 2 MW capacities respectively, are considered for the analysis here. Similarly, solar PV units with 1.0 and 1.5 MW installed capacities are used here as candidates for investment. Note that the results in the previous subsection correspond to wind and solar PV type DGs both with a 1.0 MW capacity.

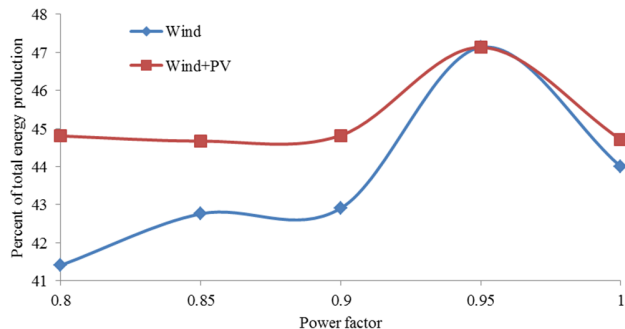


Fig. 15. Evolution of wind and solar PV energy production share with varying power factor.

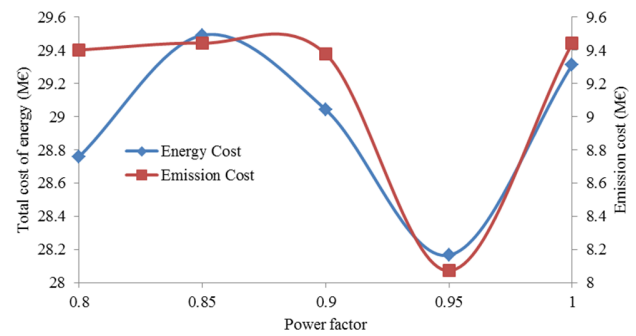


Fig. 16. Evolution of total energy and emission costs with varying power factor.

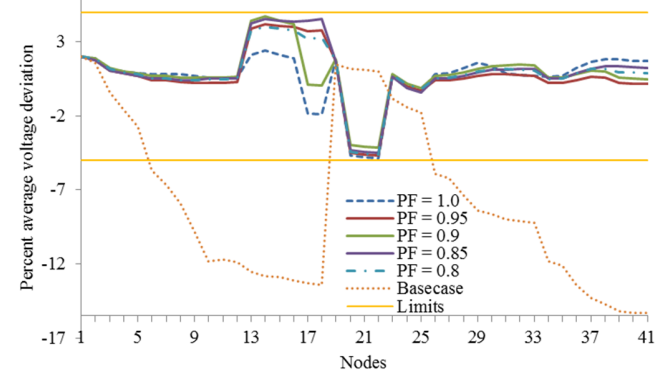


Fig. 17. Average voltage deviations at each node for different power factor values.

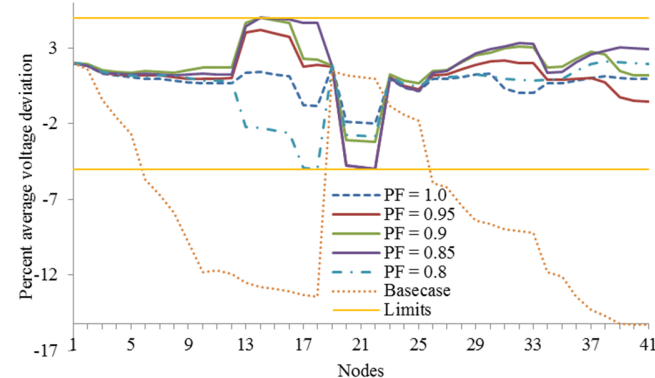


Fig. 18. Voltage deviations at each node during valley hour for different power factor values.

The results corresponding to the second case, presented here, are compared with those corresponding to the 0.95 power factor setting in Table VI, also reproduced in Table VII.

The differences in the results of both cases are visible. For instance, the total MW RES installed in the system increased from 8 MW in the previous case to 13.5 MW when wind turbines of 2.0 MW are used. As a result, the share of combined wind and solar PV energy production throughout the planning horizon is nearly 30% higher when DGs with higher capacity are installed. In addition, all cost terms and active power losses are lowered as a result of investing in DGs with higher installed capacities. Surprisingly, the storage requirement (5 MW) is significantly lower when wind turbines with higher installed capacity are used than in the other case (8 MW) as shown in Table VII, while the reactive power requirement is almost the same for both cases. The average

voltage profiles of both cases in the system are also very similar (as shown in Fig. 19).

TABLE VII

VALUES OF SYSTEM VARIABLES WITH DIFFERENT SIZES OF RES-BASED DGs			
	Wind/ solar PV size(MW)	1.0/1.0	2.0/1.5
Total energy (MWh)		179329	167330
RES energy production share (%)	Wind	47.13	59.05
	PV	0.00	1.44
	Wind+PV	47.13	60.49
Cost terms (M€)	Investment cost	33.18	37.57
	Maintenance Cost	9.98	9.85
	Emission Cost	8.07	6.67
	Energy Cost	28.17	24.36
Total cost (M€)		79.4	78.45
Investment decisions	Storage (MW)	8	5.0
	Capacitor (MVar)	3.4	3.3
	RES (MW)	8	13.5
	Line reinforcements	1	1
Average active power losses in stage 1 (MW)		0.437	0.408
Average reactive power losses in stage 1 (MVar)		0.629	0.742

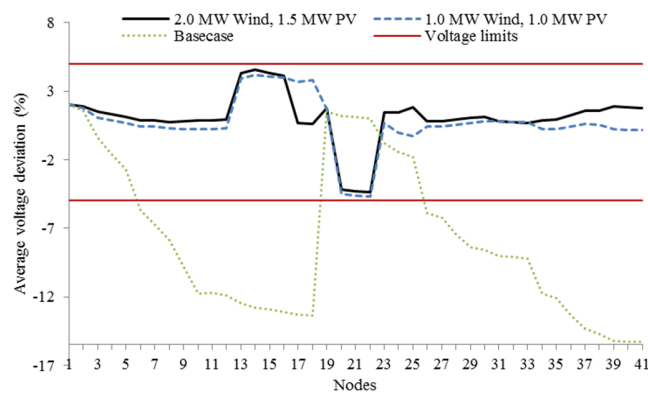


Fig. 19. Average voltage deviations at each node for different DG sizes.

IV. CONCLUSIONS

A new dynamic and stochastic mathematical model of an integrated distribution system planning problem has been proposed in Part I. To test the validity and efficiency of the proposed model, extensive numerical results and discussions of a case study have been presented, carried out on the standard IEEE 41-bus radial distribution system. The results showed that the simultaneous integration of ESSs and reactive power sources largely enabled a substantially increased penetration of variable generation (wind and solar) in the system, and consequently reduced system costs and network losses as well as deferred network expansion or reinforcement needs, which is of crucial importance. For the case study, up to 13.5 MW installed capacity of wind and solar power has been added to the system within a three-years planning horizon. One can put this into perspective with the base-case peak load of 4.635 MW in the system. This means it has been possible to integrate RES power more than twice the peak demand in the base case. Generally, it has been unequivocally demonstrated that the joint planning of DGs, reactive power sources and ESS, proposed in this work, brings about significant improvements to the system, such as reduction of losses, electricity cost and emissions. Besides, the proposed modeling framework considerably contributes to improved voltage

profile in the system. This in turn leads to an increased voltage stability margin in the system, which is essential for a normal/secure operation of the system as a whole. Overall, the novel planning model proposed here can be considered as a major leap forward towards developing controllable grids, supporting large-scale integration of RESs.

REFERENCES

- [1] M. Wang and J. Zhong, "Islanding of systems of distributed generation using optimization methodology," in *2012 IEEE Power and Energy Society General Meeting*, 2012, pp. 1–7.
- [2] M. E. Baran and F. F. Wu, "Network reconfiguration in distribution systems for loss reduction and load balancing," *Power Deliv. IEEE Trans. On*, vol. 4, no. 2, pp. 1401–1407, 1989.
- [3] F. Díaz-González, A. Sumper, O. Gomis-Bellmunt, and R. Villafañila-Robles, "A review of energy storage technologies for wind power applications," *Renew. Sustain. Energy Rev.*, vol. 16, no. 4, pp. 2154–2171, May 2012.
- [4] B. Zakeri and S. Syri, "Electrical energy storage systems: A comparative life cycle cost analysis," *Renew. Sustain. Energy Rev.*, vol. 42, pp. 569–596, Feb. 2015.
- [5] G. Munoz-Delgado, J. Contreras, and J. M. Arroyo, "Joint Expansion Planning of Distributed Generation and Distribution Networks," *IEEE Trans. Power Syst.*, vol. 30, no. 5, pp. 2579–2590, Sep. 2015.
- [6] D. Z. Fitiwi, L. Olmos, M. Rivier, F. de Cuadra, and I. J. Pérez-Arriaga, "Finding a representative network losses model for large-scale transmission expansion planning with renewable energy sources," *Energy*, vol. 101, pp. 343–358, Apr. 2016.
- [7] A. Ellis, R. Nelson, E. Von Engeln, R. Walling, J. MacDowell, L. Casey, E. Seymour, W. Peter, C. Barker, B. Kirby, and J. R. Williams, "Reactive power performance requirements for wind and solar plants," in *2012 IEEE Power and Energy Society General Meeting*, 2012, pp. 1–8.
- [8] A. Sadighmanesh, K. Zare, and M. Sabahi, "Distributed Generation unit and Capacitor Placement for Loss, Voltage profile and ATC Optimization," *Int. J. Electr. Comput. Eng. IJECE*, vol. 2, no. 6, pp. 774–780, Dec. 2012.
- [9] Jenkins, O'Malley, Fox, Bryans, Anaya-Lara, Milborrow, Watson, and Flynn, *Wind Power Integration: Connection and system operational aspects*. Institution of Engineering and Technology, 2007.



Sergio F. Santos received the B.Sc. and M.Sc. degrees from the University of Beira Interior (UBI), Covilhã, Portugal, in 2012 and 2014, respectively. He was a researcher between 2013 and 2015 in the EU FP7 Project SiNGULAR in Sustainable Energy Systems Lab of the same university. He is currently pursuing the Ph.D. degree under UBI / Santander Totta doctoral incentive grant in the Engineering Faculty in UBI. His research interests are in planning and operation optimization of distribution system and smart grid technologies integration.



Desta Z. Fitiwi received the B.Sc. degree in Electrical and Computer Engineering from Addis Ababa University, Ethiopia in 2005, M.Sc. degree in electrical and electronics engineering from Universiti Teknologi PETRONAS, Tronoh, Malaysia, in 2009. He worked as a Supervisory Control and Data Acquisition (SCADA) and Adaptation Engineer in the Ethiopian Load Dispatch Center Project from 2005 to 2007. He is pursuing an Erasmus Mundus Joint Doctorate in Sustainable Energy Technologies and Strategies (SETS), jointly offered by Comillas Pontifical University, KTH Royal Institute of Technology of Stockholm and Delft University of Technology. He actively participated in the realization of four EU-funded projects. He is currently working as a researcher at University of Beira Interior, Covilhã, Portugal. His research interests include regulation and economics of the power industry, transmission expansion planning, sustainable energy modeling and strategic planning, artificial-intelligence applications and mathematical optimizations for power systems.



Abebe W. Bizuayehu (M'15) received the M.Sc. degree in mechanical engineering, in the specialty of industrial mechanic from José Antonio Echevarría Higher Polytechnic Institute (I.S.P.J.A.E.), Havana, Cuba, in 1989, and the Ph.D. degree in Renewable Energy and Energetic Efficiency from the University of Zaragoza, Spain, in 2012. He received his postdoc from the University of Beira Interior (UBI) Covilha, Portugal in

2015, while working on the EU-funded FP7 project SiNGULAR.



Miadreza Shafie-khah (S'08, M'13) received the M.Sc. and Ph.D. degrees in electrical engineering from Tarbiat Modares University, Tehran, Iran, in 2008 and 2012, respectively. He received his first postdoc from the University of Beira Interior (UBI), Covilha, Portugal in 2015, while working on the EU-funded FP7 project SiNGULAR. He is currently pursuing his second postdoctoral studies in the University of Salerno, Salerno, Italy. His research interests include power

market simulation, market power monitoring, power system optimization, operation of electricity markets, price forecasting and smart grids.



Carlos M. P. Cabrita was born in Lisbon, Portugal on July 2, 1951. He received the E. E. Diploma and the PhD on E. E. from the Technical University of Lisbon, Lisbon, Portugal, in 1976 and 1988, respectively. He has been with Technical University of Lisbon, from 1978 to 1996. He has been with the University of Beira Interior since 1997, where he is currently Full Professor in the Department of Electromechanical Engineering. His research interests are focused on electrical machines

design and maintenance processes. He has published about 250 papers in technical journals and conference proceedings.



João P. S. Catalão (M'04-SM'12) received the M.Sc. degree from the Instituto Superior Técnico (IST), Lisbon, Portugal, in 2003, and the Ph.D. degree and Habilitation for Full Professor ("Agregação") from the University of Beira Interior (UBI), Covilha, Portugal, in 2007 and 2013, respectively.

Currently, he is a Professor at the Faculty of Engineering of the University of Porto (FEUP), Porto, Portugal, and Researcher at INESC TEC, INESC-ID/IST-UL, and C-MAST/UBI. He was the Primary Coordinator of the EU-funded FP7 project SiNGULAR ("Smart and Sustainable Insular Electricity Grids Under Large-Scale Renewable Integration"), a 5.2-million-euro project involving 11 industry partners. He has authored or coauthored more than 450 publications, including 147 journal papers, 271 conference proceedings papers, 23 book chapters, and 11 technical reports, with an *h*-index of 27 (according to Google Scholar), having supervised more than 40 post-docs, Ph.D. and M.Sc. students. He is the Editor of the books entitled *Electric Power Systems: Advanced Forecasting Techniques and Optimal Generation Scheduling* and *Smart and Sustainable Power Systems: Operations, Planning and Economics of Insular Electricity Grids* (Boca Raton, FL, USA: CRC Press, 2012 and 2015, respectively). His research interests include power system operations and planning, hydro and thermal scheduling, wind and price forecasting, distributed renewable generation, demand response and smart grids.

Prof. Catalão is an Editor of the IEEE TRANSACTIONS ON SMART GRID, an Editor of the IEEE TRANSACTIONS ON SUSTAINABLE ENERGY, and an Associate Editor of the *IET Renewable Power Generation*. He was the Guest Editor-in-Chief for the Special Section on "Real-Time Demand Response" of the IEEE TRANSACTIONS ON SMART GRID, published in December 2012, and the Guest Editor-in-Chief for the Special Section on "Reserve and Flexibility for Handling Variability and Uncertainty of Renewable Generation" of the IEEE TRANSACTIONS ON SUSTAINABLE ENERGY, published in April 2016. He was the recipient of the 2011 Scientific Merit Award UBI-FE/Santander Universities and the 2012 Scientific Award UTL/Santander Totta. Also, he has won 4 Best Paper Awards at IEEE Conferences.